Mem. S.A.It. Suppl. Vol. 22, 181

Memorie della
Supplementi

Study of the ^{2}H(α,γ)^{6}Li nuclear reaction producing ^{6}Li in standard Big Bang nucleosynthesis

Michael Anders[1], Daniel Bemmerer[1], and Carlo Gustavino[2]
for the LUNA collaboration

[1] Helmholtz-Zentrum Dresden-Rossendorf (HZDR), Dresden, Germany
e-mail: d.bemmerer@hzdr.de
[2] Istituto Nazionale di Fisica Nucleare (INFN), Sezione di Roma 1, Rome, Italy

Abstract. The ^{2}H(α,γ)^{6}Li reaction dominates the production of lithium-6 in standard Big Bang nucleosynthesis. Due to its exceedingly low cross section, this reaction has never been studied experimentally at the relevant energies, and consequently the adopted reaction rate depends on uncertain extrapolations. A direct study of the ^{2}H(α,γ)^{6}Li cross section is currently underway at the LUNA 400 kV accelerator, located deep underground in the Gran Sasso laboratory, Italy. The expected data lie directly at big-bang energies. It is hoped that they help constrain non-standard lithium-6 production scenarios, by putting the standard Big Bang production on a solid experimental footing.

Key words. Big Bang nucleosynthesis, Experimental nuclear astrophysics, ^{6}Li

1. Introduction

The ^{2}H(α,γ)^{6}Li reaction is the leading nuclear reaction producing ^{6}Li in standard Big Bang nucleosynthesis. Other reactions make only minor contributions (Serpico et al. 2004). When adopting standard nuclear reaction parameters, the predicted ^{6}Li yield is four orders of magnitude lower than the prediction for ^{7}Li, much lower than the limit of detection (Serpico et al. 2004).

However, observations of the minor lithium isotope ^{6}Li in metal-poor stars have suggested a possible cosmological ^{6}Li problem (Asplund et al. 2006), that would come in addition to the well-known cosmological ^{7}Li problem (Fields 2011, a recent review). Even though many of the claimed ^{6}Li detections may be in error (Lind et al., 2012), for a few metal-poor stars (Smith et al. 1993) there still seems to be a significant amount of ^{6}Li detectable (Steffen et al., 2012).

^{6}Li is more fragile towards nuclear reactions than its more abundant sister isotope ^{7}Li. Therefore, any detections of ^{6}Li raise the question of a possible cosmological production. However, cosmological scenarios producing enough ^{6}Li all involve non-standard physics (Kusakabe et al. 2006; Pospelov 2007; Jedamzik & Pospelov 2009; Pospelov & Pradler 2010).

Before studying such exotic scenarios, it is important to first quantify precisely how much ^{6}Li can be produced in standard Big Bang nu-

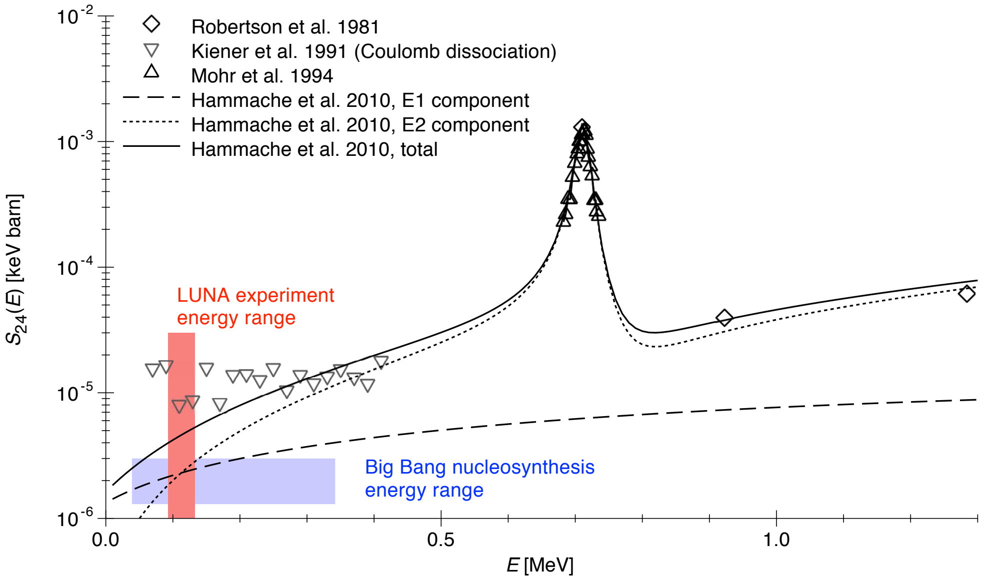

Fig. 1. State of the art for the $^2H(\alpha,\gamma)^6Li$ cross section, parameterized as the astrophysical S-factor $S_{24}(E)$. The approximate energy range of interest for Big Bang nucleosynthesis depends on the Gamow peak, i.e. the convolution of the respective energy dependences of the thermal Maxwell-Boltzmann distribution and of the cross section, and is marked in color. The energy range of the present experiment is also given. The references are discussed in the text.

cleosynthesis, to provide a firm experimental baseline how much, if any, additional ^6Li must be provided by non-standard approaches.

2. State of the art

Due to its very low value, the $^2H(\alpha,\gamma)^6Li$ cross section has never been measured experimentally at the energies relevant to Big Bang nucleosynthesis. Theoretical predictions remain uncertain (Marcucci et al. 2006), so it is necessary to constrain them by experiment. In the low-energy domain, the cross section $\sigma_{24}(E)$ is usually parameterized as the so-called astrophysical S-factor $S_{24}(E)$ defined by

$$S_{24}(E) = E\,\sigma(E)\,\exp(2\pi\eta(E)) \qquad (1)$$

with E the center-of-mass energy (throughout this text, E always denotes the center-of-mass energy, and E_α the α-beam energy in the laboratory system), and $2\pi\eta(E)$ the Sommerfeld parameter parameterizing the exponential-like energy dependence of Coulomb barrier tunneling (Rolfs & Rodney 1988). The state of the art for the S-factor $S_{24}(E)$ is plotted in fig. 1.

Two attempts to determine the $^2H(\alpha,\gamma)^6Li$ cross section have been made using the Coulomb dissociation technique (Kiener et al. 1991; Hammache et al. 2010). In this approach, the time-reversed reaction $^6Li(\gamma,\alpha)^2H$ is studied using virtual photons emitted when an energetic ^6Li beam passes close to a target of high nuclear charge. The cross section of interest is then obtained by applying the detailed balance theorem. The limits of this method lie in its predominant sensitivity to the quadrupole (E2) component of the breakup, largely neglecting the dipole component, and in the possible background from non-Coulomb, i.e. nuclear breakup.

Recently, data from the Coulomb breakup of ^6Li, studied at a ^6Li projectile energy of 150 MeV/A using the KaOS spectrometer at GSI have been published (Hammache et al. 2010). However, it was found that nu-

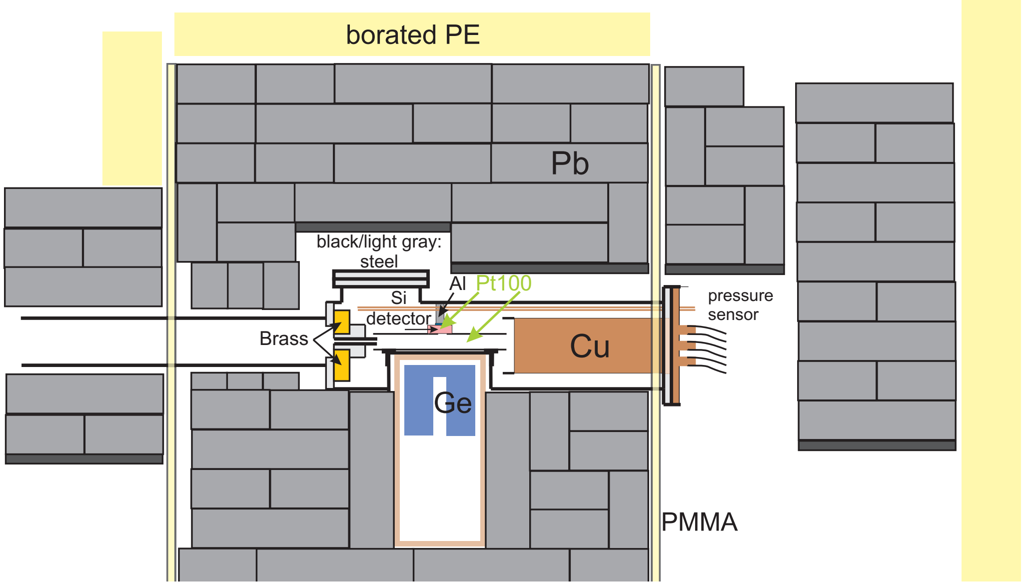

Fig. 2. Experimental setup. The central chamber of the windowless gas target is seen near the center of the plot. The α-beam enters the target from the left side through a 4 cm long collimator of 7 mm inner diameter and is stopped at the right side on a massive copper beam calorimeter. The germanium (for γ-rays) and the silicon (for particles) detectors are also shown, as well as the Pt100 temperature sensors and the flange where the capacitive pressure sensor is connected. The setup is surrounded by a lead castle and walls of borated polyethylene.

clear breakup dominated the signal, so only an experimental upper limit could be derived (Hammache et al. 2010). In addition, the angular distributions observed seemed to lend some support to a theoretical excitation function developed in the same paper. It is likely that the previous Coulomb breakup data (Kiener et al. 1991), which had been obtained at a much lower ^{6}Li projectile energy of 25 MeV/A, are even more strongly affected by nuclear breakup, so that also these data should be interpreted as upper limits (Hammache et al. 2010). So the problem remains to directly measure the ^{2}H(α,γ)^{6}Li cross section at Big Bang energies.

There are some experimental data at higher energies in the literature. The reaction has been studied previously by in-beam γ-spectrometry around the $E = 0.711$ MeV resonance (Mohr et al. 1994). At even higher energy, there are some data that have been obtained by in-beam detection of the ^{6}Li reaction products (Robertson et al. 1981). In both cases (Mohr et al. 1994; Robertson et al. 1981), an α-beam had been incident on a deuterium gas target. A third experiment at very low energy, using a deuterated polyethylene target, just resulted in an upper limit (Cecil et al. 1996).

The present work reports on the effort to complement the previous high-energy data (Mohr et al. 1994; Robertson et al. 1981) and the previous upper limits (Kiener et al. 1991; Cecil et al. 1996; Hammache et al. 2010) by experimental data directly at the energies relevant to standard Big Bang nucleosynthesis.

3. Experimental setup

3.1. The LUNA 400 kV underground accelerator

The experiment was performed at the Laboratory Underground for Nuclear Astrophysics (LUNA) 400 kV underground accelerator in the Gran Sasso laboratory, Italy. The Gran Sasso underground facility is shielded from cosmic-ray induced muons by a rock overburden equivalent to 3800 m water, reducing the muon flux by six orders of magnitude. The ambient neutron flux at Gran Sasso is of the order of $10^{-6}\,s^{-1}\,cm^{-2}$ (Belli et al. 1989; Arneodo et al. 1999), three orders of magnitude below the flux observed at the surface of the Earth.

LUNA is the world's only underground accelerator facility. It is dedicated to cross section measurements of astrophysically relevant reactions at ultra-low energy (Broggini et al. 2010). Owing to the ultra-low background observed at LUNA (Bemmerer et al. 2005; Caciolli et al. 2009; Szücs et al. 2010), a number of reactions of stellar hydrogen burning, both in the Sun and in heavier stars, have been studied at unprecedented low energies (Broggini et al. 2010; Caciolli et al. 2011; Strieder et al. 2012, to name some recent examples).

During the experiment described here, the LUNA 400 kV accelerator provided a He^+ beam of 280-400 keV energy and an intensity of 100-350 μA.

3.2. Windowless gas target system

The analyzed He^+ beam was directed to a windowless gas target system consisting of three differential pumping stages. After passing through a series of three collimators of 25, 15, and 7 mm diameter, the beam enters the target chamber proper (fig. 2). Inside the target, deuterium gas of 99.8% chemical purity and isotopic enrichment was maintained at a constant pressure of 0.3 mbar via a capacitive pressure sensor (independent of gas type, calibrated to 0.25% precision) controlling the gas inlet via a feedback loop.

Due to the efficient differential pumping system, the gas pressure outside the windowless gas target chamber was typically a factor 100 lower than inside the target. The first pumping stage was evacuated by a 2050 m^3/h roots pump, the second pumping stage by three 1500 l/s turbomolecular pumps, and the third pumping stage by a 360 l/s turbomolecular pump. The backing pumps for the three pumping stages were oil-free rotary vane compressors.

The ion beam was stopped on the thick copper head of a beam calorimeter. Resistive heaters maintained a constant temperature gradient between 70° C on the hot side, facing the beam, and 0° C on the cold side of the calorimeter.

The gas temperature inside the target chamber varied monotonously between 15° C next to the water-cooled entrance collimator and 70° C immediately adjacent to the hot side of the calorimeter. The pressure profile has been measured in a similar setup in a previous experiment at LUNA and was found to be flat (Bemmerer et al. 2006), and it is assumed here that it is flat and equal to the value measured at the pressure measurement port.

The effective target density depends on target pressure and temperature, but also on the beam heating effect. This effect has been studied previously at LUNA for ^{3}He gas, in a setup similar to the present one, by double elastic scattering (Marta et al. 2006). For ^{3}He gas, the elastic scattering data (Marta et al. 2006) are in agreement with the predicted (Osborne et al. 1984) beam heating correction ΔT from the beam current I, energy loss in the target dE/dx, heat conductivity λ and the sizes of target chamber r_{Chamber} and beam r_{Beam}

$$\Delta T = I\frac{dE}{dx}\frac{1}{2\pi\lambda}\ln\frac{r_{\mathrm{Chamber}}}{r_{\mathrm{Beam}}} \qquad (2)$$

Replacing the parameters $\frac{dE}{dx}$ and λ with the values for deuterium gas, a correction of 8-12 K is obtained, corresponding to a 3-4% reduction in effective target density. Again as in previous work (Marta et al. 2006), a conservative relative uncertainty of 40% is assumed for this correction.

3.3. Processes expected in the target

Inside the target, mainly the following nuclear reactions are expected to take place:

$$^2\mathrm{H}(\alpha,\gamma)^6\mathrm{Li} \qquad \text{(R1)}$$
$$^2\mathrm{H}(\alpha,\alpha)^2\mathrm{H} \longrightarrow {}^2\mathrm{H(d,n)}^3\mathrm{He} \qquad \text{(R2)}$$
$$\longrightarrow {}^2\mathrm{H(d,p)}^3\mathrm{H} \qquad \text{(R3)}$$

Reactions R2 and R3 are parasitic reactions induced by elastically scattered deuterons. As these deuterons have a maximum energy of only 133 keV, further deuteron-induced reactions are negligible due to suppression by the Coulomb barrier. However, there is no Coulomb barrier for the 3 MeV neutrons released by reaction R2, and the protons released by reaction R3 have an energy of up to 3 MeV. Therefore, these protons and neutrons give rise to further reactions on the structural material of the gas target system and on the detector material. The cross sections of the two parasitic reactions are similar, and they have nearly the same energy dependence at the energies relevant here (Leonard et al. 2006). Therefore, the easily detectable protons from reaction R3 my be used to approximately infer also the yield of reaction R2.

Reaction R1 is the main reaction to be studied. It gives rise to a single γ-ray at energy

$$E_\gamma = Q + E_{\mathrm{CM}} + \Delta E_{\mathrm{Doppler}} - \Delta E_{\mathrm{Recoil}} \quad (3)$$

While the γ-energy shift due to the recoiling compound nucleus is negligible here, $\Delta E_{\mathrm{Recoil}} \approx 0.2$ keV, the Doppler correction is significant, with the full Doppler shift amounting to $\Delta E_{\mathrm{Doppler}} = 16$ keV at $E_\alpha = 400$ keV. As the target is extended over the full diameter of the germanium detector leading to emissions before and behind the detector, the γ-rays fall into a region of interest that is 35 keV wide. The respective contributions of electric dipole and electric quadrupole capture to the cross section is known only from theory (Marcucci et al. 2006; Hammache et al. 2010), so the angular distribution of the emitted γ-rays is not known.

3.4. Data acquisition

The data from the germanium detector were passed on to two independent data acquisition systems for processing and storage. One branch of the data included the TNT2 digital data acquisition system in a Caen N1728B module, operated in list mode. In the second branch, histograms were recorded at regular intervals using the Ortec 919E EtherNIM analog to digital converter and multichannel buffer. The deadtime was estimated using a pulser for the TNT2 system, and using the Gedcke-Hale algorithm for the EtherNIM system. The data from the silicon detector were treated just by the Ortec branch, with a dead time estimation by a pulser connected to the preamplifier test input.

The main parameters of the gas target system and calorimeter, such as the pressures observed in the various pumping stages and the temperatures at several places inside the calorimeter, were logged at intervals of a few seconds via a Labview-based slow control system.

4. Observations with the germanium γ-ray detector

The underground location and the massive lead shielding strongly suppress the laboratory background induced by cosmic rays and by radionuclides, respectively. This makes highly sensitive experiments in principle possible (Caciolli et al. 2009). The remaining laboratory background exhibits some remaining radionuclide lines. This is mainly due to the fact that the shielding consists of only 20 cm lead for practical reasons, less than the 25 cm lead and 5 cm copper used previously Caciolli et al. (2009). Even still, the laboratory background continuum in the region of interest for the $^2H(\alpha,\gamma)^6Li$ study, at E_γ = 1585-1620 keV, is lower than the expected signal, if one assumes the cross section from the previous theoretical curve (Hammache et al. 2010) to be correct.

However, the background induced by the ion beam is formidable (fig. 3). This is mainly due to reaction R2 discussed above. This reaction gives rise to the production of about 10 neutrons of MeV energy range per second. This rather limited source rate is even lower than the already low ambient neutron flux that a setup of comparable size would be exposed to at the surface of the Earth, due to cosmic ray effects. However, in the ultra-low background setting of the LUNA facility, it proves to dominate the remaining background.

Throughout the spectrum, there are wide triangular shapes caused by (n,n'γ) processes

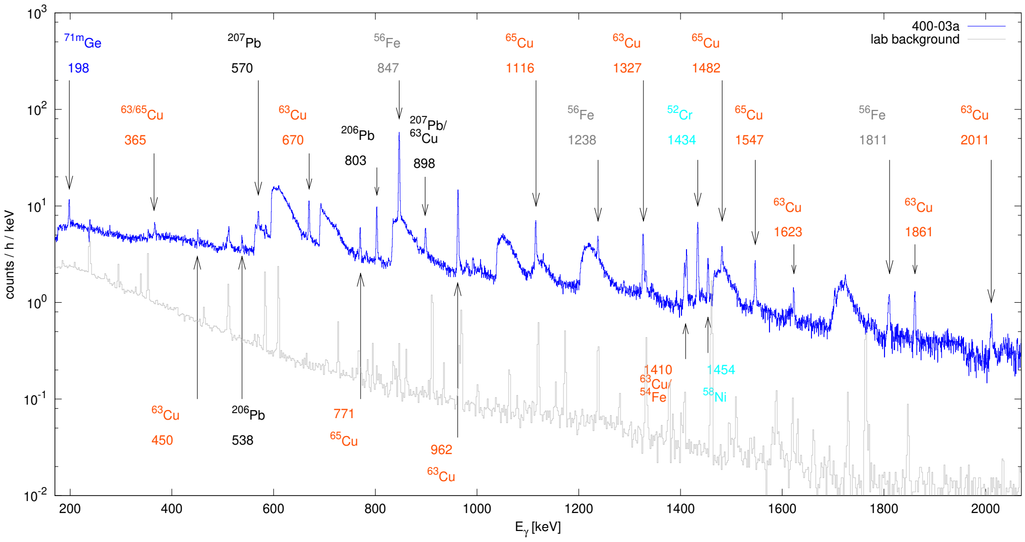

Fig. 3. Spectra taken with the germanium detector. Blue full line: in-beam spectrum at E_α = 400 keV, p_{Target} = 0.3 mbar, laboratory background subtracted. Grey thin line: Laboratory background. The most important in-beam lines due to (n,n'γ) and (n,γ) processes are marked with arrows, and the relevant target nuclide is given.

on the germanium nuclei in the detector. The energy of the triangle is given by the energy of the state being excited in the germanium nucleus, and its shape by the energy deposition of the recoiling germanium target nucleus, after correcting for quenching effects (Ljungvall & Nyberg 2005).

In addition to these large features, there are a number of sharp peaks caused by (n,γ) and (n,n'γ) processes outside the detector itself, in copper and steel parts of the setup and in the lead shielding. The nuclide responsible for these non-detector peaks is detailed in fig. 3.

All of the γ-rays emitted due to the above described processes lead not only to the full-energy peaks and triangles that can be identified in the spectrum, but also to a significant Compton continuum at lower energies. This continuum also affects the region of interest where the Doppler-shifted γ-rays from the $^2H(\alpha,\gamma)^6Li$ reaction are expected (fig. 4).

In order to derive a $^2H(\alpha,\gamma)^6Li$ cross section, this background must be subtracted. One possible method of background subtraction currently under study is to repeat the experiment at a lower beam energy, E_α = 280 keV, where the signal counting rate is expected to be three times lower. Also, the expected signal location in the γ-ray spectrum shifts downwards by 40 keV, outside the region of interest for the E_α = 280 keV run. As the energy dependences of the two processes making up background reaction (R2) are opposite, they are expected to roughly cancel out, leading to an equal background rate for the two E_α energies.

The expected very similar shape and counting rate of the background at the two energies is borne out by the data (fig. 4). There is even a hint of excess counts in the region of interest for the E_α = 400 keV run. The counting rate of this excess is roughly consistent with the previous theoretical S-factor (Hammache et al. 2010).

Whether or not this possible excess is significant, and what its precise value is, if applicable, are currently under investigation. To this end, new data are currently being taken at slightly shifted beam energies, and a detailed analysis based also on Monte Carlo simulations and on statistical tests is underway.

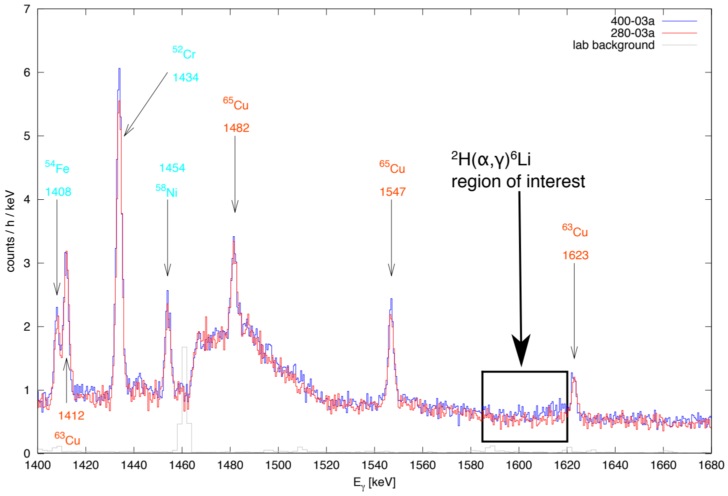

Fig. 4. Detailed view of germanium detector spectra. Blue (red) full line: in-beam spectrum at E_α = 400 keV (280 keV), p_{Target} = 0.3 mbar, laboratory background subtracted. Grey thin line: Laboratory background. The region of interest where the ^{2}H(α,γ)^{6}Li signal is expected for the E_α = 400 keV run (blue spectrum) is also marked.

5. Astrophysics implications and outlook

Already the present preliminary results clearly rule out a cosmological lithium-6 production on a level consistent with the claimed halo star lithium detections (Smith et al. 1993; Asplund et al. 2006). In order to solve the problem posed by these detections, one would have to assume a cross section value that is so high that the signal would have clearly emerged out of the present background even without any subtraction. Rather, the present data give a hint that the theory curve presented in the recent GSI Coulomb dissociation paper (Hammache et al. 2010) is at least on the correct order of magnitude.

Still, a positive value of the ^{2}H(α,γ)^{6}Li cross section at Big Bang energies would help constrain any non-standard scenario aiming to produce cosmological lithium-6. The presently described experiment is still ongoing and is hoped to provide this needed cross section value.

Acknowledgements. We thank the organizers for an interesting and stimulating workshop. — This work was supported by INFN, DFG (BE 4100/2-1), and NAVI.

References

Arneodo, F., Borio di Tigliole, A., Cavanna, F., et al. 1999, Nuovo Cimento A, 112, 819
Asplund, M., Lambert, D. L., Nissen, P. E., Primas, F., & Smith, V. V. 2006, ApJ, 644, 229
Belli, P., Bernabei, R., D'Angelo, S., et al. 1989, Nuovo Cimento A, 101, 959
Bemmerer, D., Confortola, F., Costantini, H., et al. 2006, Phys. Rev. Lett., 97, 122502
Bemmerer, D., Confortola, F., Lemut, A., et al. 2005, Eur. Phys. J. A, 24, 313
Broggini, C., Bemmerer, D., Guglielmetti, A., & Menegazzo, R. 2010, Annu. Rev. Nucl. Part. Sci., 60, 53
Caciolli, A., Agostino, L., Bemmerer, D., et al. 2009, Eur. Phys. J. A, 39, 179
Caciolli, A., Mazzocchi, C., Capogrosso, V., et al. 2011, A&A, 533, A66
Cecil, F. E., Yan, J., & Galovich, C. S. 1996, Phys. Rev. C, 53, 1967
Fields, B. D. 2011, Annu. Rev. Nucl. Part. Sci., 61, 47

Hammache, F., Heil, M., Typel, S., et al. 2010, Phys. Rev. C, 82, 065803
Jedamzik, K. & Pospelov, M. 2009, New Journal of Physics, 11, 105028
Kiener, J., Gils, H. J., Rebel, H., et al. 1991, Phys. Rev. C, 44, 2195
Kusakabe, M., Kajino, T., & Mathews, G. J. 2006, Phys. Rev. D, 74, 023526
Leonard, D. S., Karwowski, H. J., Brune, C. R., Fisher, B. M., & Ludwig, E. J. 2006, Phys. Rev. C, 73, 045801
Lind K., et al. 2012, MSAIS 22, 142
Ljungvall, J. & Nyberg, J. 2005, Nucl. Inst. Meth. A, 546, 553
Marcucci, L., Nollett, K., Schiavilla, R., & Wiringa, R. 2006, Nucl. Phys. A, 777, 111
Marta, M., Confortola, F., Bemmerer, D., et al. 2006, Nucl. Inst. Meth. A, 569, 727
Mohr, P., Kölle, V., Wilmes, S., et al. 1994, Phys. Rev. C, 50, 1543
Osborne, J., Barnes, C., Kavanagh, R., et al. 1984, Nucl. Phys. A, 419, 115
Pospelov, M. 2007, Phys. Rev. Lett., 98, 231301
Pospelov, M. & Pradler, J. 2010, Annu. Rev. Nucl. Part. Sci., 60, 539
Robertson, R. G. H. et al. 1981, Phys. Rev. Lett., 47, 1867
Rolfs, C. & Rodney, W. 1988, Cauldrons in the Cosmos (Chicago: University of Chicago Press)
Serpico, P. D., Esposito, S., Iocco, F., et al. 2004, J. Cosmol. Astropart. Phys., 2004, 010
Smith, V. V., Lambert, D. L., & Nissen, P. E. 1993, ApJ, 408, 262
Steffen M. et al., 2012, MSAIS 22, 152
Strieder, F., Limata, B., Formicola, A., et al. 2012, Phys. Lett. B, 707, 60
Szücs, T., Bemmerer, D., Broggini, C., et al. 2010, Eur. Phys. J. A, 44, 513